

# Colorimetric and Spectral Characterization of a Color Scanner Using Local Statistics

Hui-Liang Shen and John H. Xin

*Institute of Textiles & Clothing, The Hong Kong Polytechnic University, Hong Kong, China*

The accuracy of scanner characterization is usually affected by two factors. First, the statistics may vary for individual color samples and, second, the behavior of the scanner may depart from the linear reflectance model. This article proposes a method of colorimetric and spectral characterization for a color scanner using local statistics to deal with these problems. The experimental results showed that the proposed method significantly outperforms one using global statistics. The color accuracy of the colorimetric characterization is slightly better than that of the spectral one, while cross-media metamerism exists for both methods.

Journal Imaging Science and Technology 48: 342–346 (2004)

## Introduction

Recently, imaging devices such as digital cameras and scanners have become widely used in a variety of applications, and, as a consequence, the faithful exchanging of color information between different devices is becoming an important issue. The characterization establishes the relationship between the device-dependent responses and device-independent color representation, i.e., CIE tristimulus values and spectral reflectance values, of imaging devices. The colorimetric characterization has been studied extensively in the past decade, while the spectral characterization is now starting to attract attentions.<sup>1,2</sup>

Typical techniques used for colorimetric characterization are least squares based polynomial regression,<sup>3,4</sup> look-up-table with interpolation and extrapolation,<sup>5,6</sup> and artificial neural networks.<sup>7,8</sup> The polynomial regression is perhaps the most frequently adopted technique in colorimetric characterization because of its simplicity and good performance. The use of different high order terms in polynomial regression and their influence on the characterization performance were carefully studied.<sup>3,9</sup> A major drawback of the colorimetric characterization is its constraint to specific combinations of illuminant and observer functions. When either the illuminant or the observer function changes, the characterization process has to be performed again. The spec-

tral characterization recovers the spectral reflectance of a color sample from its responses produced by imaging devices. The spectral sensitivity (or responsivity) of the imaging system plays as an important role in the spectral characterization. Since it is difficult and costly to measure the spectral responsivity of a scanner, many researchers tried to recover it mathematically.<sup>10–14</sup> Based on the recovered spectral responsivity, different techniques were proposed for the spectral characterization of digital cameras and scanners.<sup>15–18</sup> A common assumption of these techniques is that the spectral sensitivities (or responsivity) of the imaging system are accurate enough. However, for a real scanner, its spectral sensitivity may considerably depart from the linear reflectance model,<sup>10</sup> and thus one cannot ensure whether those techniques still work when the mathematically recovered spectral responsivity is not accurate enough.

For both colorimetric and spectral characterization the performance is closely related to the correlation between the device responses and the device-independent measurement data of color samples. For polynomial regression, one may find that a small number of terms is insufficient to describe the total correlation of the colors, while larger number of terms may become over-fitted. This is because that the correlation cannot be described using a single transform from device responses to colorimetric values. For spectral characterization, the statistical distribution of the color samples is also important to the characterization performance as the mapping is from low dimensional device response space to high dimensional reflectance space.<sup>15,16</sup>

In this article, we propose a method of estimating colorimetric and spectral reflectance values from device responses using the local statistics of the training samples. As the behavior of scanners may depart from the linear reflectance model, spectral responsivity is not explicitly used in the spectral characterization. Instead, we establish the direct transform between scanner re-

Original manuscript received November 10, 2003

tcxinjh@inet.polyu.edu.hk; phone: +852 2766 6474; fax: +852 2773 1432

©2004, IS&T—The Society for Imaging Science and Technology

sponses of selected training samples and their corresponding CIE XYZ values (or spectral reflectance values) for colorimetric (or spectral) characterization, respectively. The experimental results showed that, in both colorimetric and spectral characterizations, the proposed method performed significantly better than the traditional ones using global statistics.

### Colorimetric and Spectral Characterization of Color Scanner

When a sample with spectral reflectance  $r(\lambda)$  is viewed under an illumination with spectral power distribution  $L_e(\lambda)$ , the CIE XYZ tristimulus values can be determined according to the color matching function  $\bar{x}(\lambda)$ ,  $\bar{y}(\lambda)$ , and  $\bar{z}(\lambda)$  in the visible spectrum range  $\Lambda$  as<sup>19</sup>

$$X = K \int_{\Lambda} L_e(\lambda) \bar{x}(\lambda) r(\lambda) d\lambda = \int_{\Lambda} h_1(\lambda) r(\lambda) d\lambda \quad (1)$$

$$Y = K \int_{\Lambda} L_e(\lambda) \bar{y}(\lambda) r(\lambda) d\lambda = \int_{\Lambda} h_2(\lambda) r(\lambda) d\lambda \quad (2)$$

$$Z = K \int_{\Lambda} L_e(\lambda) \bar{z}(\lambda) r(\lambda) d\lambda = \int_{\Lambda} h_3(\lambda) r(\lambda) d\lambda \quad (3)$$

where

$$K = 100 / \int_{\Lambda} L_e(\lambda) \bar{y}(\lambda) d\lambda \quad (4)$$

For mathematical simplicity, the continuous functions in Eqs. (1) to (4) can be represented by their sampled counterparts, and the integration can consequently be denoted as summation. If  $N$  uniformly spaced samples are used over the visible spectrum range  $\Lambda$ , Eqs. (1) to (3) can be combined and rewritten in the matrix-vector notation

$$\mathbf{x} = \mathbf{h}\mathbf{r} \quad (5)$$

where  $\mathbf{x} = [X, Y, Z]^T$  ( $T$  denotes transpose) is the vector of XYZ values,  $\mathbf{h}$  is the  $3 \times N$  matrix of  $h_k(\lambda)$  ( $k = 1, 2, 3$ ), and  $\mathbf{r}$  is the  $N \times 1$  vector of  $r(\lambda)$ .

Theoretically, for an ideal color scanner, the response of the  $k$ th ( $k = 1, 2, 3$ ) sensor at a particular pixel can be determined as<sup>20</sup>

$$\begin{aligned} v_k &= \int_{\Lambda} L_s(\lambda) k d(\lambda) r(\lambda) d\lambda + b_k + n_k \\ &= \int_{\Lambda} m_k(\lambda) r(\lambda) d\lambda + b_k + n_k \end{aligned} \quad (6)$$

where  $f_k(\lambda)$  is the spectral transmittance of the  $k$ th color filter,  $d(\lambda)$  is the spectral sensitivity of the detector in the measurement,  $L_s(\lambda)$  is the spectral radiance of the scanner illuminant,  $b_k$  is a constant bias response, and  $n_k$  is signal independent noise. As the filter transmittance, sensor sensitivity, and illuminant radiance are unknown, it is convenient to group them into one quantity  $m_k(\lambda) = f_k(\lambda) d(\lambda) L_s(\lambda)$ , which we refer to as scanner spectral responsivity in this study.

Equation (6) can also be written in its matrix vector notation as

$$\mathbf{V} = \mathbf{M}\mathbf{r} + \mathbf{b} + \mathbf{n} \quad (7)$$

where  $\mathbf{V}$  is the  $3 \times 1$  vector of  $v_k$ ,  $\mathbf{M}$  is the  $3 \times N$  matrix of  $m_k(\lambda)$ ,  $\mathbf{b}$  is the  $3 \times 1$  vector of  $b_k$ , and  $\mathbf{n}$  is the  $3 \times 1$  vector of  $n_k$ . Let  $\mathbf{U} = \mathbf{V} - \mathbf{b}$ , Eq. (7) becomes

$$\mathbf{U} = \mathbf{M}\mathbf{r} + \mathbf{n} \quad (8)$$

Practically, the actual response of a scanner  $\rho_k$  of the  $k$ th sensor is subject to a nonlinear input-output function known as optoelectronic conversion function (OECF)  $F_k$  as the following<sup>13</sup>:

$$\rho_k = F_k(v_k) \quad (9)$$

The OECF is a monotonically increasing nonlinear function that can be derived by scanning a series of gray patches.

The colorimetric characterization is to calculate the CIE XYZ values  $\mathbf{x}$  from the linear scanner responses  $\mathbf{V}$  or  $\mathbf{U}$ . Due to technical reasons such as signal-to-noise ratio (SNR) and filter design,  $\mathbf{x}$  is generally not a linear transformation of  $\mathbf{V}$  or  $\mathbf{U}$ .<sup>9</sup> Hence, the adoption of high order and cross-term in polynomial regression is necessary. Hong et al.<sup>3</sup> found that 11 polynomial terms could produce satisfactory results in digital camera characterization, while Herzog et al.<sup>9</sup> further investigated the influence of different combination of high order polynomial terms. Considering that the characterization principle of a scanner is similar to that of a digital camera, we also use second-order polynomial terms. Therefore, the colorimetric characterization is to find a  $3 \times L$  ( $L = 10$ ) matrix  $\mathbf{Q}$  to map scanner responses to CIE XYZ values:

$$\mathbf{x} = \mathbf{Q}\mathbf{g} \quad (10)$$

where

$$\mathbf{g} = [v_1, v_2, v_3, v_1^2, v_2^2, v_3^2, v_1v_2, v_1v_3, v_2v_3, 1]^T \quad (11)$$

is a polynomial term vector. Let  $\mathbf{x}_j$  and  $\mathbf{g}_j$  ( $j = 1, 2, 3, \dots$ ) be the  $j$ th CIE XYZ value and polynomial term vector of the  $j$ th training sample, respectively, then the transform matrix  $\mathbf{Q}$  can be solved using Moore–Penrose pseudo-inverse<sup>21</sup> as the following

$$\mathbf{Q} = (\mathbf{X}\mathbf{G}^T)(\mathbf{G}\mathbf{G}^T)^{-1} \quad (12)$$

where  $\mathbf{X} = [\mathbf{x}_1, \mathbf{x}_2, \mathbf{x}_3, \dots]$ , and  $\mathbf{G} = [\mathbf{g}_1, \mathbf{g}_2, \mathbf{g}_3, \dots]$ .

For spectral characterization, the convenient solution is to estimate the reflectance vector  $\hat{\mathbf{r}}$  from the linear response vector  $\mathbf{u}$  by an  $N \times 3$  matrix  $\mathbf{W}$ :

$$\hat{\mathbf{r}} = \mathbf{W}\mathbf{U} \quad (13)$$

We regard the estimation of spectral reflectance from linear response as determining the linear transform matrix  $\mathbf{W}$  in Eq. (13) such that  $\hat{\mathbf{r}}$  is a close replica of  $\mathbf{r}$  in minimum mean square error (MMSE) sense. Thus, with

$$J = E \left\{ \|\hat{\mathbf{r}} - \mathbf{r}\|^2 \right\}, \quad (14)$$

where  $E$  denotes statistical expectation operator, the problem is to determine  $\mathbf{W}$  that minimizes  $J$ . By differentiation of  $J$  with respect to  $\mathbf{W}$ , we get the Wiener–Hopf equation<sup>22</sup>

$$\mathbf{W} = \mathbf{R}_{ru} \mathbf{R}_r^{-1} \quad (15)$$

where

$$\mathbf{R}_{ru} = \mathbf{E}\{\mathbf{r}\mathbf{U}^T\}, \quad (16)$$

$$\mathbf{R}_r = \mathbf{E}\{\mathbf{r}\mathbf{r}^T\}, \quad (17)$$

are the cross- and auto-correlation matrix, respectively. Alternatively, by introducing the orthogonality principle, the calculation of transform matrix  $\mathbf{W}$  becomes<sup>23</sup>

$$\mathbf{W} = \mathbf{K}_r \mathbf{M}^T (\mathbf{M} \mathbf{K}_r \mathbf{M}^T + \mathbf{K}_n)^{-1} \quad (18)$$

where

$$\mathbf{K}_r = \langle \mathbf{r}\mathbf{r}^T \rangle \quad (19)$$

$$\mathbf{K}_n = \langle \mathbf{n}\mathbf{n}^T \rangle \quad (20)$$

with  $\langle \rangle$  being the ensemble average.<sup>22</sup> Equation (18) is widely used in multispectral imaging and spectral characterization.<sup>16,17</sup> An implicit assumption of this equation is that the spectral responsivity is accurate enough. However, for a real scanner, its behavior may depart from the linear reflectance model considerably, and thus the transform matrix  $\mathbf{W}$  should not be calculated according to Eq. (18). In this case, we consider Eq. (15) is more appropriate as it does not explicitly incorporate the spectral responsivity.

### Characterization Using Local Statistics

It is noticed that the calculation of matrix  $\mathbf{Q}$  (or  $\mathbf{W}$ ) is highly relevant to the correlation between  $\mathbf{V}$  and  $\mathbf{x}$  (or  $\mathbf{r}$ ) of the training samples. In some cases, we may be able to estimate the transform matrix  $\mathbf{Q}$  and  $\mathbf{W}$  using all the available training samples in database. More commonly, however, the statistics or correlation matrix may be considerably different for individual samples.<sup>16</sup> Hence, the global correlation matrix might be insufficient to describe the transform relationship. The feasible alternative is to calculate the local statistics using neighboring training samples instead of the global one.

It is important to decide how many training samples should be involved in the colorimetric and spectral characterization respectively. The estimation using too few training samples might be heavily biased by noise, while using too many training samples might fail to describe the local statistics accurately. If we let  $N_c$  and  $N_s$  be the number of training samples in the colorimetric and spectral characterization respectively, the problem is to decide the value of  $N_c$  and  $N_s$  so that the characterization error is considerably small.

Let the linear response of the candidate sample and the  $i$ th training sample in database be  $\mathbf{V}_t$  and  $\mathbf{V}_i$  respectively. We calculate the Euclidean distance between  $\mathbf{V}_t$  and  $\mathbf{V}_i$  in the linear *RGB* color space

$$d_i = \|\mathbf{V}_t - \mathbf{V}_i\| \quad (21)$$

Before choosing the neighboring training samples of  $\mathbf{V}_t$ , we rearrange the training samples in ascending order according to the distance  $d_i$  as  $\mathbf{V}_1^*$ ,  $\mathbf{V}_2^*$ , ...,  $\mathbf{V}_i^*$ , ..., etc.

When the training samples are not uniformly distributed in the color space, it is possible that some candidate samples have many close neighboring training samples, while some others do not. To simulate the real characterization problem, we further exclude the candidate sample  $\mathbf{V}_t$  itself in the selection of training samples. Therefore, the training samples are selected from  $\mathbf{V}_2^*$  to  $\mathbf{V}_{N_c+1}^*$  (or  $\mathbf{V}_{N_s+1}^*$ ) for colorimetric (or spectral) characterization.

### Experiments and Discussion

In the experiments, a flatbed color scanner, Epson GT-10000+, was used in characterization. Color adjustment functions of the scanner were disabled in the scanning process. The color targets used were GretagMacbeth ColorChecker Chart (MCC), GretagMacbeth ColorChecker DC (CDC), and Kodak Gray Scale Q-14 (Q14). These three color targets were scanned in at a resolution of 72 dpi. The dark color patches (A2, A5, A8, A11, etc.) of the CDC target were not used since they do not reflect enough light. The glossy ones (S1-T12) of the CDC target were also not used. For each color patch, its mean responses were calculated in a small center area so that the effect of stray light from neighboring patches can be neglected. The reflectance data of the color patches on color targets MCC, CDC, and Q14 were measured by the GretagMacbeth spectrophotometer CE-7000A across the visible spectrum from 400 to 700 nm with a sampling interval of 10 nm. Small aperture, UV and specular included measurement conditions were used. The CIE XYZ values of the color patches were calculated under illuminant D<sub>65</sub> and CIE 1931 two degree observer function.

The inverse OECF  $F_k^{-1}$  was built using the gray color patches of Q14, and then the linear responses  $\mathbf{V}$  of the color patches on the MCC were obtained according to Eq. (9) by regarding the  $F_k^{-1}$  as a one-dimensional look-up-table. Several constraints, such as smoothness, positivity, and reproduction accuracy, were introduced according to inequalities of Eqs. (22) to (24), in recovering spectral responsivity.

$$|2M_k(i) - M_k(i-1) - M_k(i+1)| \leq \varepsilon \quad (22)$$

$$\mathbf{M}_k \geq \mathbf{0} \quad (23)$$

$$|v_k - \mathbf{M}_k \mathbf{r}| \leq \delta \quad (24)$$

where  $\varepsilon = 1.0$  and  $\delta = 0.01$ ,  $\mathbf{M}_k$  is the  $k$ th ( $k = 1, 2, 3$ )  $1 \times N$  vector of matrix  $\mathbf{M}$ , and  $M_k(i)$  is the  $i$ th element of vector  $\mathbf{M}_k$ . This problem can be regarded as constrained linear least squares and can be solved using standard mathematical methods such as the routine *lsqlin* in Matlab. The solved spectral responsivity is shown in Fig. 1 and the calculated  $\mathbf{b} = [2.03, 2.41, 1.51]^T$ , using the 24 color patches on MCC. As shown, the spectral responsivity at some wavelengths is slightly below 0, which conflicts with Eq. (23). This is due to the over stringent constraints with the inequalities<sup>22-24</sup> for the scanner used, and the spectral responsivity shown in Fig. 1 is the optimal solution under these constraints. Nevertheless, the shape of the responsivity seems quite reasonable. We simulated the linear response of MCC and CDC using the measured reflectance data and the recovered  $\mathbf{M}$  according to Eq. (9) by assuming the noise vector  $\mathbf{n} = [0, 0, 0]^T$ . The errors between actual and simulated linear responses are shown in Table I. It can be seen that the errors of the blue channel are slightly larger than those of the red and green channels. In addition, the mean and standard deviation of the absolute errors of the test target CDC are approximately two times larger than those of MCC. This clearly indicates that the recovered spectral responsivity is not accurate enough. It is considered that the scanner departs from the linear reflectance model as the errors for some color patches are relatively high. Therefore, as expected, the recovered  $\mathbf{M}$  should not be used in Eq. (18) for spectral reflectance estimation.

**TABLE I.** Comparison of the actual linear responses  $V_k$  and predicted ones  $\hat{V}_k$  using mathematically recovered spectral responsivity. The error of a color is calculated using  $|V_k - \hat{V}_k|/V_{k,max} \times 100\%$ , where  $V_{k,max}$  is the maximum linear response of the  $k$ th channel of the white patch of MCC.

	MCC			CDC		
	Red	Green	Blue	Red	Green	Blue
Mean error (%)	0.80	0.75	1.41	1.88	1.66	2.78
Maximum error (%)	1.90	1.56	4.65	4.70	5.05	9.69

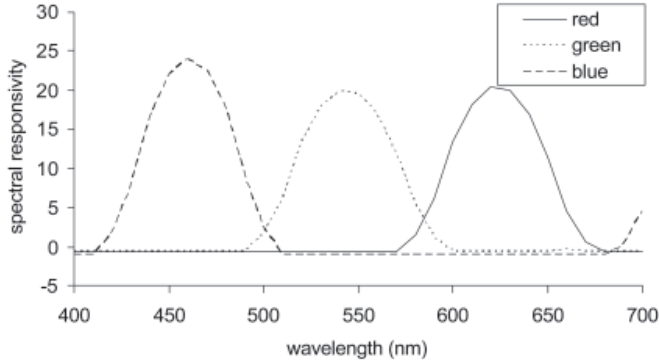


**Figure 1.** Recovered spectral responsivity of the scanner using color patches on MCC.

The colors on the target CDC were used as the training sample database. The mean CIE 1994 color difference  $\Delta E_{94}^*$  under standard illuminant  $D_{65}$  for different values of  $N_c$  and  $N_s$  were plotted in Fig. 2. It was found that in both colorimetric and spectral characterization, the mean color difference decreases first and then increase steadily with the increasing of the number of training samples. It was considered that  $N_c = 40$  and  $N_s = 20$  is appropriate for the target CDC in this study. The value of  $N_c$  and  $N_s$  may be different when different color targets, as the selection of training samples are related to the color distribution in color space.

The colorimetric and spectral characterization were conducted for CDC using local statistics ( $L_c = 40$  and  $L_s = 20$ ) and global statistics. For spectral characterization, its accuracy can be evaluated using the spectral root mean square (SRMS) error defined as follows:

$$\text{SRMS error} = \left[ \frac{(\mathbf{r} - \hat{\mathbf{r}})^T (\mathbf{r} - \hat{\mathbf{r}})}{N} \right]^{1/2}. \quad (25)$$

An alternative metric is to calculate the color difference  $\Delta E_{94}^*$  under various illuminants such as CIE D65, CIE A and CIE F2. The evaluation results are given in Table II. It is found that in either color difference or SRMS error, the local method significantly outperforms the global one. For colorimetric characterization, since it is constrained to a single illuminant, only the  $\Delta E_{94}^*$  of illuminant CIE D65 was calculated and illustrated in Table III. Again, the characterization results using local statistics are better than the ones using global sta-

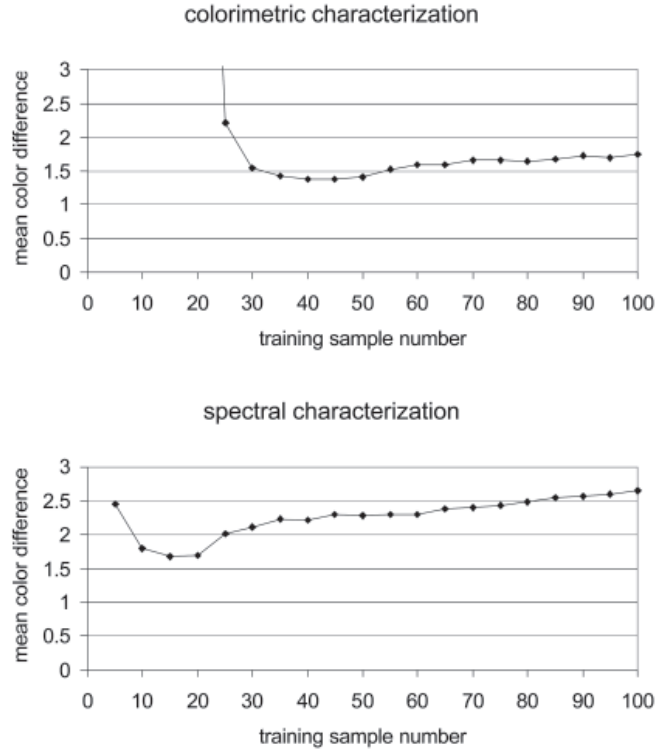


**Figure 2.** Relationship between the mean color difference  $\Delta E_{94}^*$  under  $D_{65}$  illuminant and the number of training samples in colorimetric (top) and spectral characterization (bottom) for target CDC.

tistics. From Tables II and III, the mean and standard deviation of color difference of the colorimetric characterization are lower than for the spectral one in all cases. This is due to the reason that the former maps low dimensional color space to low dimensional color space, while the latter maps low dimensional color space to high dimensional spectral reflectance. The transform of the latter is therefore much more likely to suffer from the inconsistent statistics of the training samples. The main advantage of the spectral characterization over the colorimetric one is that it is not constrained to single observer and illuminant.

In addition to testing the characterization performance on CDC itself, it is also of interest to evaluate the cross-media metamerism between different color targets such as MCC. From Tables II and III, the color differences of both the spectral and colorimetric characterizations using different color targets are considerably larger than those using the same targets. This observation is expected in the spectral characterization, since the transform from spectral reflectance to device response is a many-to-one problem. That is, given a low dimensional device response  $\mathbf{U}$ , it is usually insufficient to reconstruct its corresponding high dimensional spectral reflectance  $\mathbf{r}$  accurately. However, as pointed out by Sharma and Wang,<sup>24</sup> when the domain of the spectral reflectance is restricted to the same media, the spectral characterization becomes a one-to-one problem, and the accurate reconstruction of spectral reflectance is possible. For the colorimetric characterization, as the color matching function  $\mathbf{h}$  of human eye and the spectral responsivity  $\mathbf{M}$  of scanner is always not the same, two color patches producing the same  $RGB$  values will pro-

**TABLE II. Mean, standard deviation (Std.), and maximum (Max.) of color difference under various illuminants, and SRMS error for the spectral characterization when using local and global statistics. The training samples were from CDC, and the testing sample were from CDC (same targets) and MCC (different targets), respectively.**

Method	Metrics	Same targets			Different targets		
		Mean	Std.	Max.	Mean	Std.	Max.
Spectral (Global)	CIE D65 $\Delta E_{94}^*$	3.14	2.41	14.76	4.18	3.14	14.67
	CIE A $\Delta E_{94}^*$	2.44	2.30	9.65	3.86	4.31	15.97
	CIE F2 $\Delta E_{94}^*$	3.27	2.89	14.18	4.48	3.62	15.63
	SRMS error	0.027	0.022	0.149	0.041	0.021	0.099
Spectral (Local)	CIE D65 $\Delta E_{94}^*$	1.76	1.34	6.54	3.45	2.22	9.30
	CIE A $\Delta E_{94}^*$	1.19	0.96	4.78	3.17	3.03	13.81
	CIE F2 $\Delta E_{94}^*$	1.63	1.32	7.66	3.19	2.15	9.03
	SRMS error	0.018	0.017	0.093	0.029	0.012	0.058

**TABLE III. Mean, standard deviation (Std.), and maximum (Max.) of  $\Delta E_{94}^*$  under D65 illuminant for the colorimetric characterization when using local and global statistics. The training samples were from CDC, and the testing sample were from CDC (same targets) and MCC (different targets), respectively.**

Method	Same targets			Different targets		
	Mean	Std.	Max.	Mean	Std.	Max.
Colorimetric (Global)	2.69	2.48	10.48	4.07	3.50	13.88
Colorimetric (Local)	1.37	1.24	9.45	3.26	2.54	11.09

duce different CIE XYZ tristimulus values. This observation is also noticed by Hong et al.<sup>3</sup>

## Conclusions

In this article, we proposed a method of colorimetric and spectral characterization using local statistics of training samples. The colorimetric characterization is based on polynomial regression, while the spectral characterization is based on a minimum mean square error criterion without the explicit use of spectral responsivity. This method is considered to be applicable to real scanners, as their behavior may depart from the linear reflectance model, and the statistics may be different for individual color samples. The experimental results show that the proposed method significantly outperforms the traditional ones using global statistical information. In addition, the performance of the colorimetric characterization is slightly better than that of spectral characterization in terms of mean color difference. Nevertheless, the mean error for both of them are below 1.7  $\Delta E_{94}^*$ , which is considered to be sufficient for many applications. The characterization was also evaluated by using training samples on CDC and testing

samples on MCC. It is noted that, due to the cross-media metamerism, the proposed characterization method is not generic, but limited to single media.  $\blacktriangle$

**Acknowledgment.** The authors would like to acknowledge the financial support of this project from the Hong Kong Polytechnic University and the Research Grants Council of Hong Kong SAR Government (project reference: PolyU 5153/01E).

## References

1. R. Bala, Device characterization, in *Digital Color Imaging Handbook*, G. Shama, Ed., CRC Press, New York, 2003, pp. 269–384.
2. T. Johnson, Methods for characterizing colour scanners and digital cameras, *Displays* **16**, 183–191 (1996).
3. G. W. Hong, M.R. Luo and P.A. Rhodes, A study of digital camera colorimetric characterization based on polynomial modeling, *Color Res. Appl.* **26**, 76–84 (2001).
4. H. R. Kang, Color scanner calibration, *J. Imaging Sci. Technol.* **36**, 162–170 (1992).
5. P. C. Hung, Colorimetric calibration for scanners and media, *Proc. SPIE* **1448**, 164–174 (1991)
6. P. C. Hung, Colorimetric calibration in electronic imaging devices using a look-up-table in interpolations, *J. Electronic Imaging* **2**, 53–61 (1993).
7. H. R. Kang and P.G. Anderson, Neural network applications to the color scanner and printer calibrations, *J. Electronic Imaging* **1**, 125–134 (1992).
8. S. Tominaga, A neural network approach to color reproduction in color printers, *Proc. 1st IS&T/SID Color Imaging Conference*, IS&T, Springfield, VA, 1993, pp. 173–177.
9. P. G. Herzog, D. Knipp, H. Stiebig, and F. Konig, Colorimetric characterization of novel multiple-channel sensors for imaging and metrology, *J. Electronic Imaging* **8**, 342–353 (1999).
10. J. E. Farrell and B. A. Wandell, Scanner linearity, *J. Electronic Imaging* **2**, 225–230 (1993).
11. G. Sharma and H. J. Trussell, Set theoretic estimation in color scanner characterization, *J. Electronic Imaging* **5**, 479–489 (1996).
12. K. Barnard and B. Funt, Camera characterization for color research, *Color Res. Appl.* **27**, 152–163 (2002).
13. P. L. Vora, J. E. Farrell, J.D. Tietz, and D.H. Brainard, Image capture: simulation of sensor responses from hyperspectral images, *IEEE Trans. Image Processing* **10**, 307–316 (2001).
14. M. Thomson and S. Westland, Colour-imager characterization by parametric fitting of sensor responses, *Color Res. Appl.* **26**, 442–449 (2001).
15. M. Shi and G. Healey, Using reflectance models for color scanner calibration, *J. Opt. Soc. Amer. A*, **19**, 645–656 (2002).
16. J. M. Dicarolo and B. A. Wandell, Spectral estimation theory: beyond linear but before Bayesian, *J. Opt. Soc. Amer. A*, **20**, 1261–1270 (2003).
17. H. Haneishi, T. Hasegawa, A. Hosoi, Y. Yokoyama, N. Tsumura, and Y. Miyake, System design for accurately estimating the spectral reflectance of art paintings, *Appl. Opt.* **39**, 6621–6632 (2000).
18. F.H. Imai and R.S. Berns, A comparative analysis of spectral reflectance estimation in various spaces using a trichromatic camera system, *J. Imaging Sci. Technol.* **44**, 280–287 (2000).
19. G. Wyszecki and W. Stiles, *Color Science: Concepts and Methods, Quantitative Data and Formulae*, Wiley, New York, 1982.
20. G. Sharma and H.J. Trussell, Digital color imaging, *IEEE Trans. Image Processing* **6**, 901–932 (1997).
21. M. T. Heath, *Scientific Computing: An Introduction Survey*, 2nd ed., McGraw Hill, New York, 2002.
22. M. H. Hayes, *Statistical Digital Signal Processing and Modeling*, John Wiley & Sons Inc., New York, 1996.
23. W. K. Pratt, *Digital Image Processing*, 2nd ed., John Wiley & Sons Inc., New York, 1991.
24. G. Sharma and S. Wang, Spectrum recovery from colorimetric data for color reproductions, *Proc. SPIE* **4663**, 8–14 (2002).